Technische Universität Ilmenau
Institut für Mathematik

Preprint No. M 05/05

Pneumatic cylinders: modelling and feedback force-control

Ilchmann, Achim; Sawodny, Oliver; Trenn, Stephan

Mai 2005

Impressum:
Hrsg.: Leiter des Instituts für Mathematik
Weimarer Straße 25
98693 Ilmenau
Tel.: +49 3677 69 3621
Fax: +49 3677 69 3270
http://www.tu-ilmenau.de/ifm/

ISSN xxxx-xxxx

ilmedia

Pneumatic cylinders: modelling and feedback force-control

Achim Ilchmann* **Oliver Sawodny†** **Stephan Trenn⋆**

2 May 2005

Abstract

In this paper, we model, analyze, and control an experimental set-up of a servo pneumatic cylinder. The dynamic behaviour of pneumatic actuator systems is dominant by nonlinear functions. First, a mathematical model for the pneumatic system is derived. Secondly, we investigate the mathematical properties of this model and show boundedness and positiveness of certain variables. Thirdly, we prove that a proportional output feedback controller with saturation achieves practical tracking a wide class of reference trajectories. We verify the theoretical results and the effectiveness of the control by experiments.

Keywords: force control, pneumatic cylinder, modelling, tracking

1 Introduction

In this paper, we model, analyse, and control an experimental set-up of a pneumatic actuator as illustrated in Figure 1.

Pneumatic actuators are widely used in industrial automation, such as robotics [6], [9]. The main advantage of these actuators are low costs and high power/weight ratio. Up to now,

*Institut für Mathematik, Technische Universität Ilmenau, Weimarer Straße 25, 98693 Ilmenau, DE; achim.ilchmann@tu-ilmenau.de, stephan.trenn@tu-ilmenau.de

†Institut für Automatisierung und Systemtechnik, Technische Universität Ilmenau, POBox 100565, 98693 Ilmenau, DE; oliver.sawodny@tu-ilmenau.de

adequate applications are mostly control tasks with modest requirements on position and force accuracy; the configuration consists of binary switching valves with pneumatic cylinders without any sensor elements. To enlarge the field of applications and allowing for higher accuracy, servo pneumatic valves and sensor for pressure position have been introduced. However, if more accuracy on the performance is required, then nonlinear behaviour has to be taken into account. Most contributions in this context focus on position control: Feedback linearization as control design method is broadly used [18], [2], [19], and since in this case the relative degree is lower than the system order, the cylinder chamber pressure [18], [2] has to be measured or the zero dynamics have to be compensated by feedforward compensation [11]. As an alternative for control of pneumatic actuators, fuzzy methods [10], [13], [12], neural networks [16], and genetic algorithms [4] have been suggested. Linearization [14], [17] and linearization along reference trajectories [1] complete the control methods. Robust control approaches extend the applied control techniques [5].

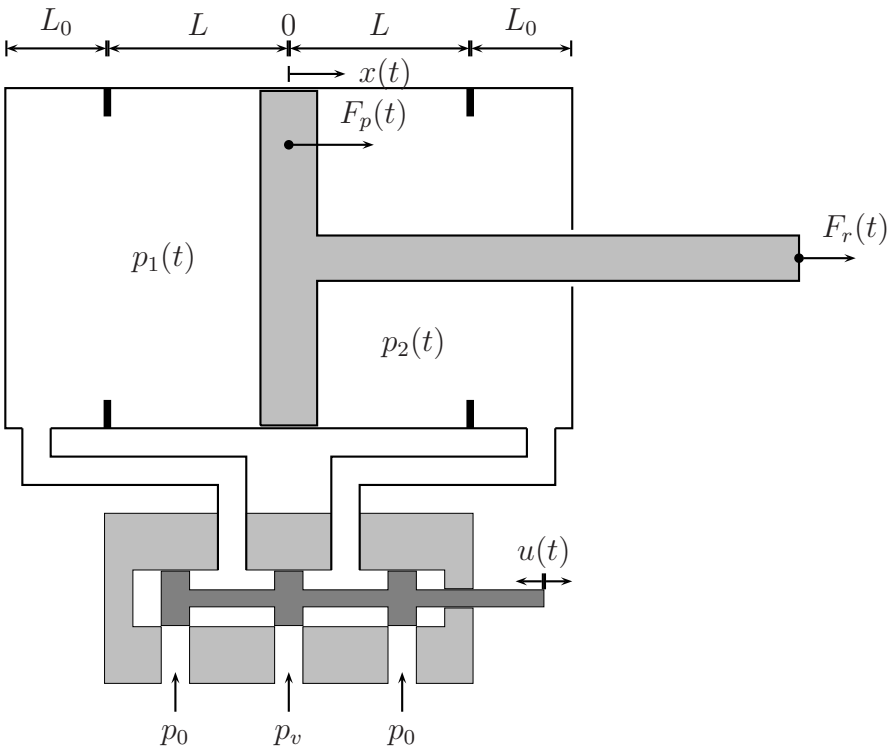

Figure 1: The pneumatic cylinder

Fewer contributions focus on force control [3]. However, no matter whether position or force control is considered, the dominant nonlinearities are in the pneumatic part, and not in the mechanical part of the system. There is a fundamental need for a detailed modelling of the dynamic behaviour of the pneumatic actuator system. A first approach is introduced by [7]. This allows to derive system theoretic properties of the model which then lead to effective

control strategies for the force control, such as force control of the inner part of the cascaded control concept.

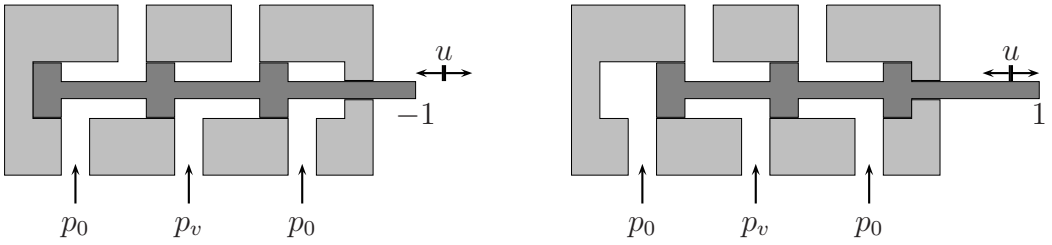

Figure 2: Operation modes of the 3/5-servo-valve

The paper is organized as follows. In Section 2, a mathematical model of a pneumatic cylinder is derived. Basic mathematical properties verifying the intuition of the model are shown in Section 3. In Section 4, a proportional output error controller with saturation is introduced; tracking and robustness properties of this controller are proved. Finally, in Section 5 we present experimental results which verify the mathematical results and show effectiveness of the control strategy.

The meaning of the symbols in Figure 1 are:

$p_1(t), p_2(t)$	pressure at time $t \geq 0$ in left/right chamber, resp.,
$x(t)$	position of the piston at time $t \geq 0$,
$F_p(t)$	pressure force on the piston at time $t \geq 0$,
$F_r(t)$	resulting force at time $t \geq 0$,
p_v	supply pressure,
p_0	ambient pressure,
$b \in (0,1)$	critical pressure fraction,
$L > 0$	$[-L, L]$ normal operation range of the cylinder,
$L_0 > 0$	additional length of piston, zone of end of travel absorbers

In addition, we close this introduction with some remarks on notation:

$A_1, A_2 > 0$	cross sectional area left/right to the piston, resp.,
$C_m > 0$	flow rate coefficient,
ρ_0	standardized density measured in kg/m^3 at temperature 293 K,
$\kappa > 0$	adiabatic exponent,
$R > 0$	ideal gas constant,
$T > 0$	temperature in Kelvin,
$v(t)$	velocity of the piston, i.e. $v = \dot{x}$
$a(t)$	acceleration of the piston, i.e. $a = \ddot{x}$
$\dot{m}(p, u)$	mass flow rate, see (3)

$\mathbb{R}_{\geq 0}$ $:= [0, \infty)$

$\mathbb{B}_\varepsilon(x^0)$ $:= \{x \in \mathbb{R}^n | \, \|x - x^0\| < \varepsilon\}$,
i.e. the open ball of radius $\varepsilon > 0$ centred at $x^0 \in \mathbb{R}^n$

$\partial\mathbb{B}$ the set of all boundary points of the set $\mathbb{B} \subset \mathbb{R}^n$

$\bar{\mathbb{B}}$ the closure of the set $\mathbb{B} \subset \mathbb{R}^n$

$\|x\|_\infty$ the supremum norm of a function x

$C(I; \mathbb{R}^N)$ set of continuous functions $I \to \mathbb{R}^n$, $I \subset \mathbb{R}$ an interval,

$C^1(I; \mathbb{R}^N)$ set of continuously differentiable functions $I \to \mathbb{R}^N$, $I \subset \mathbb{R}$ an interval.

2 Model of a pneumatic actuator system

The aim of the present note is to control a desired force F_p on the piston rod by the pressures p_1 and p_2 in two cylinder chambers, see Figure 1. The pressures p_1 and p_2 are measured by two pressure sensors. The force on the piston F_p depends on the effective cross section areas A_1 and $A_2 \leq A_1$ in the cylinder chambers, i.e.

$$F_p(t) = A_1 p_1(t) - A_2 p_2(t).$$

Note that due to friction effects, the resulting force F_r on the piston rod is not identical to the force F_p. However, in this paper we focus on the pneumatic dynamics and on controlling F_p.

To control the force F_p, i.e. the pressure difference, the differential cylinder is connected with a 3/5-servo-valve. The notation of 3/5 means, that the valve has three different modes of operation and five ports (one for the supply pressure p_v, two for the ambient pressure p_0, and two for the chambers of the cylinder). Between these three modes one may change continuously. The first mode is the zero-position of the valve as depicted in Figure 1; the second mode is filling chamber 1 and exhausting chamber 2 simultaneously; the third operation mode is deaerating chamber 1 and filling chamber 2. It will be assumed that the control input u is standardized such that $u = -1$ corresponds to maximum flow-rate filling chamber 2 and for $u = 1$ vice versa (see Figure 2).

The mechanical dynamics are described by

$$\left.\begin{array}{rcll} \dot{x} & = & v, & x(0) = x_0 \in [-L, L], \\ \dot{v} & = & a, & v(0) = v_0 \in \mathbb{R}, \end{array}\right\} \tag{1}$$

where x is the position, v the velocity and a the acceleration of the piston. We assume that the force compensation, which determines a, is realized such that

$$x(t) \in [-L, L] \quad \forall\, t \geq 0.$$

This assumption may be justified by the size of the cylinder and - possibly - an action of an external position controller; which is typically satisfied in such applications as assembling by force fitting.

The pressure in the cylinder chambers can be modelled [2, 8], invoking the principles of constant mass and conservation of energy, by the following differential equation:

$$\left.\begin{aligned} \dot{p_1} &= \tfrac{\kappa}{A_1(L_0+L+x)}\big(RT\,\dot{m}(p_1,u) - p_1 A_1 \dot{x}\big), \\ \dot{p_2} &= \tfrac{\kappa}{A_2(L_0+L-x)}\big(RT\,\dot{m}(p_2,-u) + p_2 A_2 \dot{x}\big)\,. \end{aligned}\right\} \tag{2}$$

The mass flow rate $\dot{m}$ depends on the flow rate function of the servo valve. The mass flow can be assumed to be a flow of a compressible fluid in a turbulent regime through a conical nozzle. In case of filling the cylinder chamber, a characteristic depending on the pressure ratio and gas flow rate is described by a square root function. Let $b \in (0,1)$ be the critical pressure fraction and define

$$\Psi_b \colon [0,1] \to [0,1], \quad q \mapsto \begin{cases} 1, & q \le b, \\ \sqrt{1 - \left(\frac{q-b}{1-b}\right)^2} & q \ge b. \end{cases}$$

Neglecting the leakage of the valve, the mass flow rate can be described by the following equation [1, 11] (see also Figure 3):

$$\dot{m} \colon \mathbb{R}_{>0} \times [-1,1] \to \mathbb{R}, \quad (p,u) \mapsto \begin{cases} -\rho_0 C_m\, p\, \Psi_b(p_v/p)\, u, & \text{if } u > 0,\ p \ge p_v, \\ \rho_0 C_m\, p_v\, \Psi_b(p/p_v)\, u, & \text{if } u > 0,\ p \le p_v, \\ 0, & \text{if } u = 0, \\ \rho_0 C_m\, p\, \Psi_b(p_0/p)\, u, & \text{if } u < 0,\ p \ge p_0, \\ -\rho_0 C_m\, p_0\, \Psi_b(p/p_0)\, u, & \text{if } u < 0,\ p \le p_0. \end{cases} \tag{3}$$

The combined mechanical and pneumatic model with feedback control is shown in Figure 4.

3 Properties of the model

In this section, we investigate the properties of the open-loop system model. It will be shown that without further assumptions, the differential equation has a unique solution with properties ensuring correct modelling; for example, the variables of the pressure stay positive and bounded.

We first consider the situation when the piston does not move.

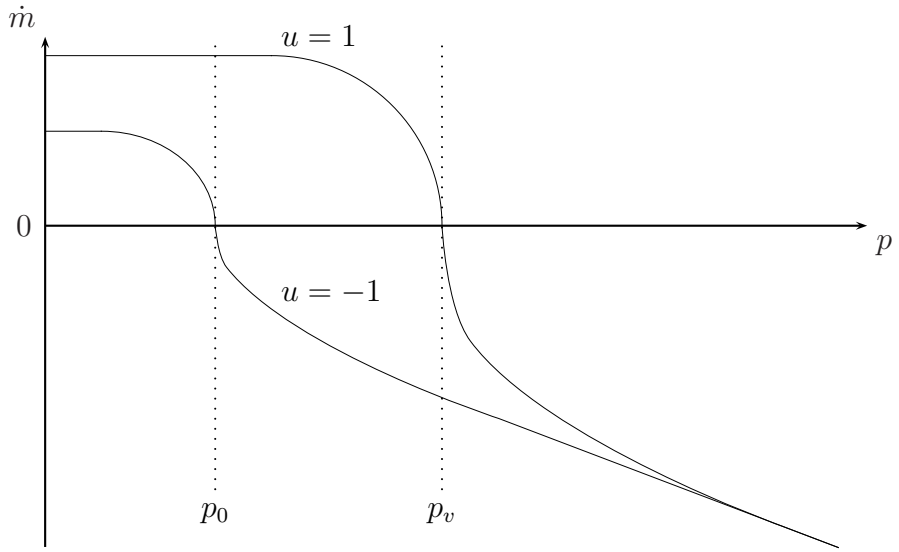

Figure 3: Qualitative behaviour of the mass flow rate $\dot{m}$.

Proposition 3.1 *Suppose that* (1) *satisfies* $v \equiv \dot{x} \equiv 0$ *and* $x \equiv x_0 \in [-L, L]$. *Then, for every piecewise continuous input* $u\colon \mathbb{R}_{\geq 0} \to [-1, 1]$ *and any initial data* $(p_1^0, p_2^0) \in [p_0, p_v] \times [p_0, p_v]$, *the initial value problem* (2), $\big(p_1(0), p_2(0)\big) = (p_1^0, p_2^0)$ *has a unique solution*

$$(p_1, p_2)\colon \mathbb{R}_{\geq 0} \to [p_0, p_v] \times [p_0, p_v]\,.$$

Proof: Existence and uniqueness of a maximally extended solution $(p_1, p_2)\colon [0, \omega) \to \mathbb{R}^2$ to (2) for some $\omega \in (0, \infty]$ follows from the theory of ordinary differential equations (e.g. Theorem 54 in [15]). We will show that $p_1(t), p_2(t) \in [p_0, p_v]$ for all $t \in (0, \omega)$; which then implies, by maximality of ω, that $\omega = \infty$.

We consider different cases for $p_1(t), p_2(t)$ with respect to p_0, p_v. First, suppose that $p_1(t) > p_v$ for some $t \in (0, \omega)$. Since $p_1(0) \leq p_v$, there exists t_0 such that $0 \leq t_0 < t$, $p_1(t_0) = p_v$ and $p_1(\tau) \geq p_v$ for all $\tau \in (t_0, t)$. By (3), it follows that, for every $u \in [-1, 1]$ and $\tau \in (t_0, t)$, we have $\dot{m}\big(p_1(\tau), u\big) \leq 0$. Hence, by invoking (2), $\dot{x} \equiv 0$, and $\dot{p}_1(\tau) \leq 0$ for all $\tau \in (t_0, t)$, we arrive at the contradiction

$$0 < p_1(t) - p_1(t_0) = \int_{t_0}^{t} \dot{p}_1(\tau) \mathrm{d}\tau \leq 0.$$

The other three cases $p_1(t) < p_0$, $p_2(t) > p_v$ and $p_2(t) < p_0$ are treated analogously and the proofs are omitted. This completes the proof of the proposition. □

The result of Proposition 3.1 is, from a physical point of view, not surprising: it confirms that the pressures in the chambers cannot become larger than the supply pressure p_v and

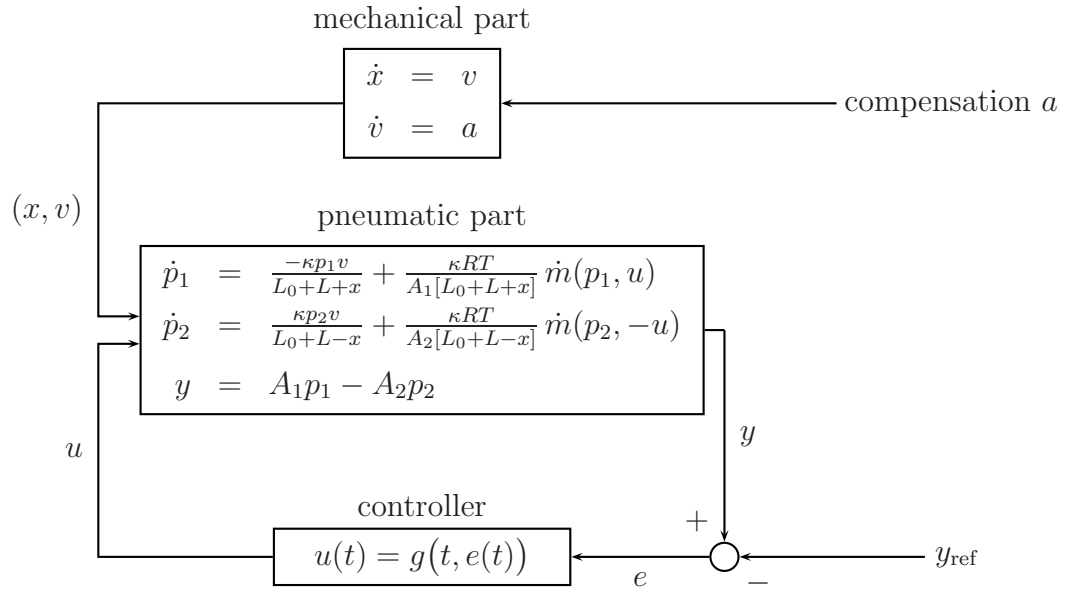

Figure 4: The model of the piston control

not smaller than the ambient pressure p_0.

The next proposition considers the more general case where movement of the piston is allowed and the control input is any piecewise continuous function. Under these rather weak assumptions it still holds that the pressures stay bounded and positive.

Proposition 3.2 *Consider* (1) *for some locally integrable function* $a\colon \mathbb{R}_{\geq 0} \to \mathbb{R}$ *such that* $x(t) \in [-L, L]$ *for all* $t \geq 0$. *Then, for every initial value* $(p_1^0, p_2^0) \in \mathbb{R}^2_{>0}$ *and for every piecewise continuous input* $u\colon \mathbb{R}_{\geq 0} \to [-1, 1]$, *there exists a unique solution to the initial value problem* (2), $\big(p_1(0), p_2(0)\big) = (p_1^0, p_2^0)$; *and this solution*

$$(p_1, p_2)\colon \mathbb{R}_{\geq 0} \to \mathbb{R}_{>0} \times \mathbb{R}_{>0}$$

is bounded and has positive values only.

Proof: Let $u\colon \mathbb{R}_{\geq 0} \to [-1, 1]$ be piecewise continuous and $(p_1^0, p_2^0) \in \mathbb{R}^2_{>0}$. Then existence and uniqueness of a maximally extended solution $(p_1, p_2)\colon [0, \omega) \to \mathbb{R}_{>0} \times \mathbb{R}_{>0}$ to the initial value problem (2), $\big(p_1(0), p_2(0)\big) = (p_1^0, p_2^0)$, for some $\omega \in (0, \infty]$, follows from the theory of ordinary differential equations (e.g. Theorem 54 in [15]).

We show boundedness of p_1 and p_2 from above on $[0, \omega)$.
Suppose there exists $\tau > 0$ such that $p_1(\tau) > \max\{p_v, p_1^0\}$. Note that if this is not satisfied, then p_1 is bounded. We may choose an interval $[\sigma, \tau] \subseteq [0, \omega)$ such that

$$p_1(\sigma) = \max\{p_v, p_1^0\} \quad \text{and} \quad p_1(t) \geq \max\{p_v, p_1^0\} \quad \forall\, t \in [\sigma, \tau].$$

Then

$$\dot{m}(p_1(t), u) \leq 0 \quad \forall\, t \in [\sigma, \tau]\ \forall\, u \in [-1, 1]\,,$$

and therefore

$$\dot{p}_1(t) \leq \frac{-\kappa v(t)}{L_0 + L + x(t)} p_1(t) \quad \forall\, t \in [\sigma, \tau],$$

whence

$$p_1(\tau) \leq e^{-\int_\sigma^\tau \frac{\kappa v(s)}{L_0+L+x(s)} \mathrm{d}s}\ \max\{p_v, p_1^0\}.$$

In passing, observe that

$$\begin{aligned} -\int_\sigma^\tau \frac{\kappa v(s)}{L_0 + L + x(s)} \mathrm{d}s \ &= \ -\kappa \ln \frac{1}{L_0 + L + x(\tau)} - \kappa \ln \frac{1}{L_0 + L + x(\sigma)} \\ &= \ \kappa \ln \frac{L_0 + L + x(\tau)}{L_0 + L + x(\sigma)}. \end{aligned} \tag{4}$$

Now in view of $x(t) \in [-L, L]$ for all $t \geq 0$,

$$p_1(t) \leq \left(\frac{L_0 + 2L}{L_0} \right)^\kappa \max\{p_v, p_1^0\} \quad \forall\, t \in [\sigma, \tau]$$

and hence p_1 is bounded from above on $[0, \omega)$. Using the same reasoning, boundedness of p_2 can be shown.

We show that (p_1, p_2) is bounded away from zero.
Suppose there exists $\tau > 0$ such that $p_1(\tau) < \min\{p_0, p_1^0\}$. We may choose an interval $[\sigma, \tau] \subseteq [0, \omega)$ so that

$$p_1(\sigma) = \min\{p_0, p_1^0\} \quad \text{and} \quad 0 < p_1(t) \leq \min\{p_0, p_1^0\} \quad \forall\, t \in [\sigma, \tau].$$

Then

$$\dot{m}(p_1(t), \operatorname{sgn} u) \geq 0 \quad \forall\, t \in [\sigma, \tau]\ \forall\, u \in [-1, 1]\,,$$

and therefore

$$\dot{p}_1(t) \geq -\frac{\kappa v(t)}{L_0 + L + x(t)}\, p_1(t) \quad \forall\, t \in [\sigma, \tau],$$

whence

$$p_1(\tau) \geq e^{-\int_\sigma^\tau \frac{\kappa v(s)}{L_0+L+x(s)} \mathrm{d}s}\ \min\{p_0, p_1^0\}.$$

Next, invoking (4) and the fact that $x(t) \in [-L, L]$ for all $t \geq 0$, yields

$$p_1(t) \geq \left(\frac{L_0}{L_0 + 2L} \right)^\kappa \min\{p_v, p_1^0\} \quad \forall\, t \in [\sigma, \tau]\,,$$

and hence p_1 is bounded away from zero on $[0,\omega)$. Similarly, it can be shown that p_2 is bounded away from zero. Hence $\omega=\infty$ and the proof is complete. □

Remark 3.3 *If $(p_1^0,p_2^0)\in[p_0,p_v]\times[p_0,p_v]$, then the proof of Proposition 3.2 shows that*

$$\left(\frac{L_0}{L_0+2L}\right)^{\kappa} p_0 \le p_i(t) \le \left(\frac{L_0+2L}{L_0}\right)^{\kappa} p_v \qquad \forall\, t\ge 0,\ \ i=1,2.$$

The following lemma shows that if the distance of $(p_1(t),p_2(t))$ to the point (p_v,p_0), measured by the distance function

$$d_{(q_1,q_2)}(p_1,p_2) := \big\|(p_1,p_2)-(q_1,q_2)\big\|_2^2 \qquad \text{for}\ \ p_1,p_2,q_1,q_2>0, \tag{5}$$

is not zero and if the input signal is positive, then this distance is decreasing (under the assumption that the "disturbance" v is sufficiently small).

Lemma 3.4 *Let $(p_1^0,p_2^0)\in\mathbb{R}_{>0}\times\mathbb{R}_{>0}$, $u\colon\mathbb{R}_{\ge0}\to[-1,1]$ a piecewise continuous function, $v\colon\mathbb{R}_{\ge0}\to\mathbb{R}$ a continuous function such that $\dot x = v$ and $x(t)\in[-L,L]$ for all $t\ge0$. Consider the unique solution $(p_1,p_2)\colon\mathbb{R}_{\ge0}\to\mathbb{R}_{>0}\times\mathbb{R}_{>0}$ to the initial value problem (2), $\big(p_1(0),p_2(0)\big)=(p_1^0,p_2^0)$. Then for every $\varepsilon>0$ and $u_0>0$, there exist $\delta_v=\delta_v(\varepsilon,u_0)>0$ and $\delta=\delta(\varepsilon,u_0)>0$ such that, for all $t\ge0$, the following implications hold:*

$$\begin{aligned}
\Big[u(t)\ge u_0 \,\wedge\, d_{(p_v,p_0)}(p_1(t),p_2(t))\ge\varepsilon \,\wedge\, |v(t)|\le\delta_v\Big] \quad&\Longrightarrow\quad \frac{d}{dt}\,d_{(p_v,p_0)}\big(p_1(t),p_2(t)\big)\le-\delta\,,\\
\Big[u(t)\le -u_0 \,\wedge\, d_{(p_0,p_v)}(p_1(t),p_2(t))\ge\varepsilon \,\wedge\, |v(t)|\le\delta_v\Big] \quad&\Longrightarrow\quad \frac{d}{dt}\,d_{(p_0,p_v)}\big(p_1(t),p_2(t)\big)\le-\delta\,.
\end{aligned} \tag{6}$$

Proof: Consider the solution (p_1,p_2) given in the statement of the lemma, suppose $u(t)\ge u_0$ for some $t\ge0$. Then (2) gives

$$\begin{aligned}
\frac{d}{dt}\,d_{(p_v,p_0)}\big(p_1(t),p_2(t)\big) &= 2(p_1(t)-p_v)\dot p_1(t)+2(p_2(t)-p_0)\dot p_2(t)\\
&= \frac{2\kappa RT}{A_1[L_0+L+x(t)]}\big(p_1(t)-p_v\big)\dot m\big(p_1(t),u(t)\big)\\
&\quad+\frac{2\kappa RT}{A_2[L_0+L-x(t)]}\big(p_2(t)-p_0\big)\dot m\big(p_2(t),-u(t)\big)\\
&\quad+\left(-\frac{2(p_1(t)-p_v)p_1(t)\kappa}{L_0+L+x(t)}+\frac{2(p_2(t)-p_0)p_2(t)\kappa}{L_0+L-x(t)}\right)v(t).
\end{aligned}$$

By Proposition 3.2, the number

$$p_{\max} \;:=\; \max\big\{\|\big(p_1(\tau),p_2(\tau)\big)\|\big|\;\tau\geq 0\big\} \;>\; 0 \tag{7}$$

is well defined, and hence we may define

$$M_1 := \max_{\substack{x\,\in\,[-L,\,L]\\ p_1,\,p_2\,\in\,[0,\,p_{\max}]}} \left|\frac{-2(p_1-p_v)p_1\kappa}{L_0+L+x}+\frac{2(p_2-p_0)p_2\kappa}{L_0+L-x}\right|.$$

For $\varepsilon>0$ let $\big(p_1^\varepsilon(t),p_2^\varepsilon(t)\big)$ be the projection of $\big(p_1(t),p_2(t)\big)$ onto the circle around (p_v,p_0) with radius $\varepsilon>0$, i.e.

$$\big(p_1^\varepsilon(t),p_2^\varepsilon(t)\big) := (p_v,p_0)+\varepsilon\,\frac{\big(p_1(t),p_2(t)\big)-(p_v,p_0)}{d_{(p_v,p_0)}\big(p_1(t),p_2(t)\big)}\,.$$

By properties of $\dot m$ (see Figure 3), it is easy to see that

$$\begin{aligned}\big(p_1(t)-p_v\big)\,\dot m\big(p_1(t),u(t)\big) \;&\leq\; \big(p_1^\varepsilon(t)-p_v\big)\,\dot m\big(p_1^\varepsilon(t),u_0\big) \;\leq\; 0 \qquad\text{and}\\ \big(p_2(t)-p_0\big)\,\dot m\big(p_2(t),-u(t)\big) \;&\leq\; \big(p_2^\varepsilon(t)-p_0\big)\,\dot m\big(p_2^\varepsilon(t),-u_0\big) \;\leq\; 0\,.\end{aligned}$$

Hence

$$\delta_1 := -\max_{\substack{x\,\in\,[-L,\,L]\\ (p_1^\varepsilon,\,p_2^\varepsilon)\,\in\,\partial\mathbb{B}_\varepsilon(p_v,\,p_0)}} \left(\frac{2\kappa RT\big(p_1^\varepsilon-p_v\big)\dot m\big(p_1^\varepsilon,u_0\big)}{A_1[L_0+L+x]}+\frac{2\kappa RT\big(p_2^\varepsilon-p_0\big)\dot m\big(p_2^\varepsilon,-u_0\big)}{A_2[L_0+L-x]}\right)\geq 0,$$

and

$$\frac{d}{dt}\,d_{(p_v,p_0)}\big(p_1(t),p_2(t)\big) \;\leq\; -\delta_1+M_1\,|v(t)|.$$

We will show that $\delta_1>0$.
Seeking a contradiction, suppose that $\delta_1=0$. Then there exist $p_1^\varepsilon,p_2^\varepsilon\in\partial\mathbb{B}_\varepsilon(p_v,p_0)$ such that

$$\big(p_1^\varepsilon-p_v\big)\,\dot m\big(p_1^\varepsilon,u_0\big)=0 \qquad\text{and}\qquad \big(p_2^\varepsilon-p_0\big)\,\dot m\big(p_2^\varepsilon,-u_0\big)=0\,.$$

By properties of $\dot m$ (see Figure 3), this is only possible if $p_1^\varepsilon=p_v$ and $p_2^\varepsilon=p_0$, which contradicts $(p_1^\varepsilon,p_2^\varepsilon)\in\partial\mathbb{B}_\varepsilon(p_v,p_0)$. Therefore, $\delta_1>0$.

The second implication in (6) follows analogously; so there exist $\delta_2>0$ and $M_2>0$ such that

$$\frac{d}{dt}\,d_{(p_0,p_v)}\big(p_1(t),p_2(t)\big) \;\leq\; -\delta_2+M_2\,|v(t)|\,.$$

For any $\delta_v\in\Big(0,<\min\Big\{\frac{\delta_1}{M_1},\frac{\delta_2}{M_2}\Big\}\Big)$, and $\delta:=\min\{\delta_1-\delta_vM_1,\delta_2-\delta_vM_2\}>0$ we have , for $|v(t)|<\delta_v$,

$$\frac{d}{dt}\,d_{(p_0,p_v)}\big(p_1(t),p_2(t)\big)<-\delta \quad\text{and}\quad \frac{d}{dt}\,d_{(p_v,p_0)}\big(p_1(t),p_2(t)\big)<-\delta, \quad\text{resp.}$$

This completes the proof of the lemma. □

The following corollary, an immediate consequence of Lemma 3.4, highlights an important property of the model, reflecting the following physical property: if $u(t) \geq u_0 > 0$ for all $t \geq 0$, then the pressures $p_1(t)$ and $p_2(t)$ converge to p_v and p_0 as $t \to \infty$, resp.

Corollary 3.5 *Consider* (2) *with initial values* $(p_1^0, p_2^0) \in \mathbb{R}_{>0} \times \mathbb{R}_{>0}$, $u\colon \mathbb{R}_{\geq 0} \to [-1,1]$ *a piecewise continuous function, and* $v \equiv 0$, *i.e.* $x(t) = x_0 \in [-L, L]$ *for all* $t \geq 0$. *Let* $(p_1, p_2)\colon \mathbb{R}_{\geq 0} \to \mathbb{R}_{>0} \times \mathbb{R}_{>0}$ *denote the unique solution to the initial value problem* (2), $\big(p_1(0), p_2(0)\big) = (p_1^0, p_2^0)$. *Then the following implications hold, for every* $u_0 > 0$*:*

$$\Big[\, \exists t_0 > 0 \,\forall\, t \geq t_0 :\ u(t) \geq u_0 \,\Big] \quad \Rightarrow \quad \lim_{t\to\infty} \big(p_1(t), p_2(t)\big) = (p_v, p_0),$$

$$\Big[\, \exists t_0 > 0 \,\forall\, t \geq t_0 :\ u(t) \leq -u_0 \,\Big] \quad \Rightarrow \quad \lim_{t\to\infty} \big(p_1(t), p_2(t)\big) = (p_0, p_v)\,.$$

4 Force control

In this section, it will be shown that the output, for cross sectional areas $A_1, A_2 > 0$ of the piston,

$$y(t) = A_1 p_1(t) - A_2 p_2(t) \qquad \forall\, t \geq 0, \tag{8}$$

in combination with the simple proportional feedback controller, for $k > 0$, with saturation

$$u(t) = \mathrm{sat}_{[-1,1]}\big(-k\, e(t)\big) \quad \text{with} \quad e(t) := y(t) - y_{\mathrm{ref}}(t) \quad \forall\, t \geq 0, \tag{9}$$

achieves practical tracking in the following sense.

Theorem 4.1 *Define*

$$Q_\gamma := [p_0 - \gamma, p_v + \gamma] \times [p_0 - \gamma, p_v + \gamma] \qquad \textit{for } \gamma \geq 0\,, \tag{10}$$

and let

$$y_{ref} \in C^1\big(\mathbb{R}_{\geq 0}; [\underline{y}, \overline{y}]\big)\,, \quad \textit{where} \quad \underline{y} := A_1 p_0 - A_2 p_v, \quad \overline{y} := A_1 p_v - A_2 p_0\,.$$

Assume that $\dot{x} = v \in C(\mathbb{R}_{\geq 0}, \mathbb{R})$ *such that* $x(t) \in [-L, L]$ *for all* $t \geq 0$. *Let* $\lambda > 0$ *and* $k \geq 1/\lambda$. *Then there exist* $\gamma > 0$ *and* $\delta_v = \delta_v(\lambda, \gamma) > 0$, $\varepsilon = \varepsilon(\lambda, \gamma) > 0$, *and* $t_0 = t_0(\lambda, \gamma) \geq 0$ *such that the solution* (p_1, p_2) *of the closed-loop system* (2), (8), (9) *satisfies*

$$\Big[\, \|\dot{y}_{ref}\|_\infty \leq \varepsilon \ \wedge\ \|v\|_\infty < \delta_v \ \wedge\ \forall\, t \geq 0 \ :\ \big(p_1(t), p_2(t)\big) \in Q_\gamma \,\Big]$$

$$\Longrightarrow \qquad \forall\, t \geq t_0 :\ |y(t) - y_{ref}(t)| \leq \lambda\,.$$

The amplitude of y_{ref} is restricted in terms of the cross section areas and the supply and ambient pressure. If the rectangular $[p_0, p_v] \times [p_0, p_v]$ is enlarged by $\gamma > 0$ to Q_γ, then for reference signals with sufficiently small change and sufficiently small disturbance of the piston, it is ensured that the proportional output error with saturation (9) keeps the error $y(t) - y_{\text{ref}}(t)$ within the interval $[-\lambda, \lambda]$. Note that the smaller $\lambda > 0$, the larger $k \geq 1/\lambda$ and the harder the restrictions by ε and δ_v; the latter becomes clear in the proof.
The crucial assumption in the implication in Theorem 4.1 is that $((p_1(t), p_2(t)) \in Q_\gamma$ for all $t \geq 0$. However, in many applications the pressures involve in Q_0 anyway.

For the proof of Theorem 4.1 we introduce the notation, for some $C \subseteq \mathbb{R}^n$

$$C_\gamma := \bigcup_{x \in C} \overline{\mathbb{B}}(x, \gamma)\,, \qquad \gamma > 0, \tag{11}$$

and state the following lemma.

Lemma 4.2 *Consider a continuous function $f\colon \mathbb{R}^n \to \mathbb{R}^n$, $n \in \mathbb{N}$, let $a \in \mathbb{R}^n$, and $C \subset \mathbb{R}^n$ be compact. Then the following implication holds for every $c_1 > 0$ and every $c_2 \in (0, c_1)$:*

$$\big[\, \forall\, x \in C :\, \langle a\,,\, f(x)\rangle \geq c_1 \,\|f(x)\| \,\big] \quad \Longrightarrow \quad \big[\, \exists \gamma > 0\, \forall\, x \in C_\gamma :\, \langle a\,,\, f(x)\rangle \geq c_2 \,\|f(x)\| \,\big],$$

Proof: The proof follows from continuity of f and compactness of C. □

Proof of Theorem 4.1: For notational convenience set $e(t) = y(t) - y_{\text{ref}}(t)$. Let (p_1, p_2) denote the solution of the closed-loop system (2), (8), (9) under the assumptions as specified in the proposition. We proceed in several steps.

Step 1: We show that if $|e(0)| < \lambda$, then there exists $t_0 \geq 0$ such that $|e(t_0)| \leq \lambda$.
Consider first the case that $|e(0)| < -\lambda$. Seeking a contradiction suppose $e(t) < -\lambda$ for all $t \geq 0$ (and hence, in particular, $u \equiv 1$). A simple geometric observation (see Figure 5) shows that for $d_{(p_v,p_0)}$ as defined in (5) we have

$$d_{(p_v,p_0)}\big(p_1(t), p_2(t)\big) \;>\; \cos(\alpha)\,\lambda/A_2 \qquad \forall\, t \geq 0, \quad \text{where } \alpha := \arctan \frac{A_1}{A_2}. \tag{12}$$

Now since $u \equiv 1$ we may apply Lemma 3.4 to conclude the existence of $\delta_v > 0$ and $\delta > 0$ such that

$$\|v\|_\infty \leq \delta_v \qquad \Longrightarrow \qquad \forall\, t \geq 0 :\; \frac{d}{dt}\, d_{(p_v,p_0)}\big(p_1(t), p_2(t)\big) \leq -\delta\,.$$

Hence there exists $t_1 > 0$ such that $d_{(p_v,p_0)}\big(p_1(t), p_2(t)\big) = 0$, which contradicts (12).

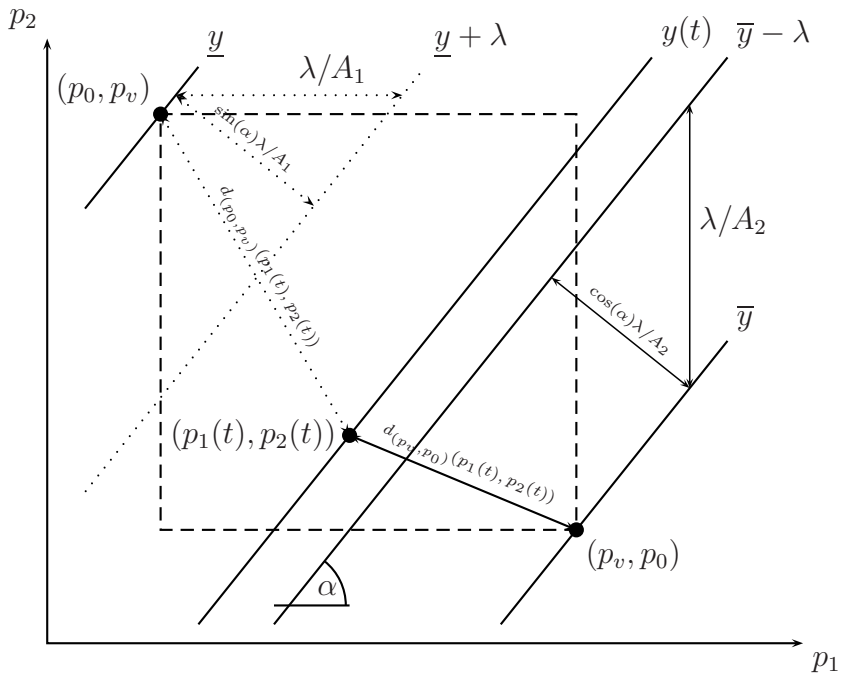

Figure 5: Geometric observation

The case $e(0) > \lambda$ is proved analogously to Step 1, the corresponding geometrical observations are illustrated with dotted lines in 5. The proof is omitted.

STEP 3: We show that if $|e(t)| = \lambda$ for some $t \geq 0$, then $\operatorname{sgn}\big(e(t)\big)\dot{e}(t) < 0$.
Let $e(t) = -\lambda$ for some $t \geq 0$. Then, by (9), $u(t) = 1$. Since $y(t) \leq \bar{y} - \lambda$, we derive, again by geometric observation as in Step 2, that

$$d_{(p_v,p_0)}\big(p_1(t), p_2(t)\big) \;\geq\; \cos(\alpha)\,\lambda/A_2.$$

Thus, by Lemma 3.4, there exist $\delta_v^1, \delta > 0$, both of which are independent of t, such that

$$\|v\|_\infty \leq \delta_v^1 \qquad \Longrightarrow \qquad \frac{d}{dt}\, d_{(p_v,p_0)}\big(p_1(t), p_2(t)\big) \leq -\delta\,.$$

Using $p_{\max}$ introduced in (7) together with the Cauchy-Schwartz inequality yields

$$\begin{aligned}\delta &\le \left| \frac{d}{dt}\, d_{(p_v,p_0)}\big(p_1(t),p_2(t)\big)\right| = 2\,\left|\Big\langle \big(p_1(t)-p_v,p_2(t)-p_0\big)^T, \big(\dot p_1(t),\dot p_2(t)\big)^T\Big\rangle\right| \\ &\le 2\,\big\|\big(p_1(t)-p_v,p_2(t)-p_0\big)\big\|\;\big\|\big(\dot p_1(t),\dot p_2(t)\big)\big\| \\ &\le 2\sqrt{2}\,p_{\max}\big\|\big(\dot p_1(t),\dot p_2(t)\big)\big\|\,,\end{aligned}$$

or, equivalently,

$$\big\|\big(\dot p_1(t),\dot p_2(t)\big)\big\| \;\ge\; \delta/(2\sqrt{2}p_{\max}) > 0. \tag{13}$$

For $x\in[-L,L]$, write

$$f_x\colon \mathbb{R}_{>0}\times\mathbb{R}_{>0}\to\mathbb{R}_{>0}\times\mathbb{R}_{>0},\quad (p_1,p_2)\mapsto \left(\frac{\kappa RT\dot m(p_1,1)}{A_1(L_0+L+x)},\,\frac{\kappa RT\dot m(p_2,-1)}{A_2(L_0+L-x)}\right)^T.$$

Since $f_x(p_1,p_2)$ and $(A_1,-A_2)^T$ lie in the same quadrant, there exists $c_1>0$ (independent of x) such that

$$\Big\langle \big(A_1,-A_2\big)^T,\, f_x(p_1,p_2)\Big\rangle \ge c_1\,\|f_x(p_1,p_2)\| \qquad \forall\,(p_1,p_2)\in Q:=[p_0,p_v]\times[p_0,p_v].$$

Now by Lemma 4.2, there exist $c_2>0$ and $\gamma>0$ such that, for Q_γ as defined (10),

$$\left\langle \begin{pmatrix} A_1\\ -A_2\end{pmatrix},\, f_x(p_1,p_2)\right\rangle \ge c_2\,\|f_x(p_1,p_2)\| \qquad \forall\,(p_1,p_2)\in Q_\gamma\,. \tag{14}$$

Since

$$\begin{pmatrix}\dot p_1(t)\\ \dot p_2(t)\end{pmatrix} = f_x(p_1(t),p_2(t)) + v(t)\,\begin{pmatrix} -\frac{p_1(t)\kappa}{L_0+L+x(t)}\\ \frac{p_2(t)\kappa}{L_0+L-x(t)}\end{pmatrix},$$

it follows from (13) that there exists $\delta_v^2\in(0,\delta_v^1)$ and $\hat\delta>0$ such that

$$|v(t)|\le\delta_v \quad\Longrightarrow\quad \|f_x(p_1(t),p_2(t))\|\ge\hat\delta>0\,. \tag{15}$$

Finally, applying (14) and (15) to

$$\begin{aligned}\dot y(t) &= \left\langle \begin{pmatrix} A_1\\ -A_2\end{pmatrix}, \begin{pmatrix}\dot p_1(t)\\ \dot p_2(t)\end{pmatrix}\right\rangle \\ &= \left\langle \begin{pmatrix} A_1\\ -A_2\end{pmatrix},\, f_x(p_1(t),p_2(t))\right\rangle + v(t)\left\langle \begin{pmatrix} A_1\\ -A_2\end{pmatrix},\, \begin{pmatrix} -\frac{p_1(t)\kappa}{L_0+L+x(t)}\\ \frac{p_2(t)\kappa}{L_0+L-x(t)}\end{pmatrix}\right\rangle,\end{aligned}$$

yields the existence of $\varepsilon > 0$ and $\delta_v \in (0, \delta_v^2)$ such that

$$|v(t)| < \delta_v \quad \Longrightarrow \quad \dot{y}(t) > \varepsilon \,,$$

and therefore,

$$|\dot{y}_{\mathrm{ref}}(t)| \leq \varepsilon \wedge |v(t)| < \delta_v \quad \Longrightarrow \quad \dot{e}(t) = \dot{y}(t) - \dot{y}_{\mathrm{ref}}(t) > 0,$$

which proves $\operatorname{sgn}\big(e(t)\big)\dot{e}(t) < 0$.

If $e(t) = \lambda$, then $y(t) \geq \underline{y} + \lambda$ and by analogous reasoning as above we may conclude that $\operatorname{sgn}\big(e(t)\big)\dot{e}(t) < 0$.

Step 4: By Step 1–3 it follows that $[-\lambda, \lambda]$ is an attractive positive-invariant region for evolution of e. This completes the proof of the proposition. □

5 Experimental set-up and measurement results

The results of the previous sections have been verified by measurements using the experimental set-up depicted in Figure 6. A pneumatic cylinder of the manufacturer *Festo* has been used; the constants given in the table at the end of the Introduction are for this cylinder as follows: $p_v = 6000$ hPa, $p_0 = 1000$ hPa, $b = 0.3$, $L = 50$ mm, $L_0 = 5$ mm, $A_1 = \pi(d_1/2)^2$ and $A_2 = A_1 - \pi(d_2/2)^2$, (where $d_1 = 25$ mm and $d_2 = 10$ mm), $C_m = 2.64 * 10^{-9}$ l/(s Pa), $\rho = 1.185$ kg/m^3, $\kappa = 1$, $R = 287$ Nm/(kg K), $T = 293$ K.

Two pressure sensors measure the chamber pressure p_1 and p_2; the position x of the piston rod is measured by a potentiometer. According to (9), the output $y(t)$ is a linear combination of the two pressures. Since the pressure measurement is corrupted by measurement noise, we implemented a low-pass filter of first order with the transfer function $s \mapsto (1 + 2s/(\pi f))^{-1}$ and cut-off frequency $f = 20$ Hz. Control and measurement data processing is implemented in Matlab/Simulink. The Simulink structure is downloaded via the Realtime Workshop to the controller board *DS1103* of the manufacturer *dspace*.

All experiments illustrate how the feedback controller (8), (9) achieves tracking of given reference trajectories as predicted in Theorem 4.1. Moreover, we also show how the controller compensates disturbances on the position of the piston rod and how it follows piecewise constant reference forces; note that the latter cases are not covered by the theoretical results. We apply the force control law (9) with gain parameter $k = 0.02$, i.e. $\lambda = 50$, and the experiments have a duration of 40 seconds. Certainly, the figures also show that the measurement data contain "real world" noise.

In Experiment 1, a continuously differentiable reference signal y_{ref} as depicted in Figure 7 is used. The piston rod is fixed mechanically and so its position is constant (i.e. the piston

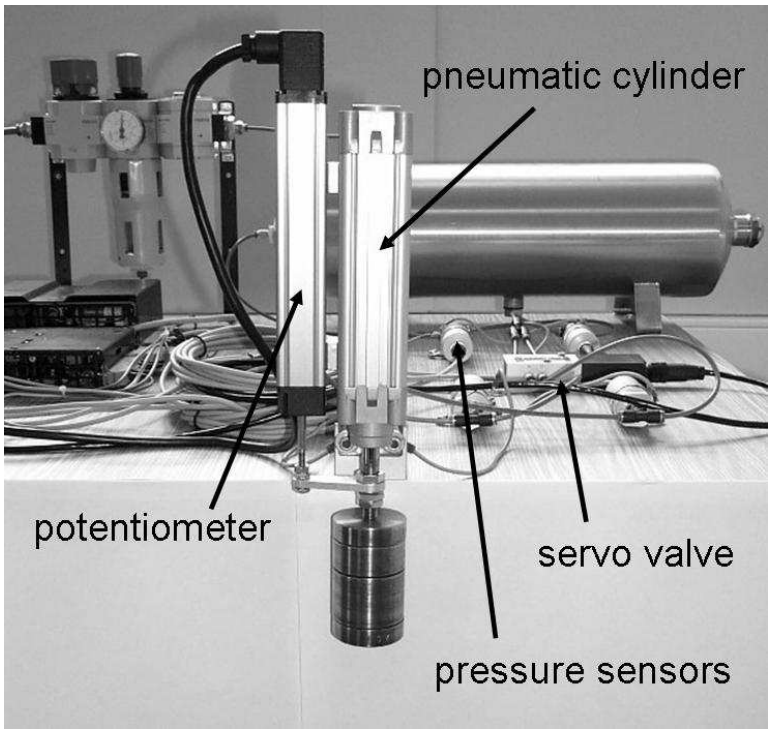

Figure 6: Experimental set-up.

velocity $v \equiv 0$). As can be seen in Figure 7, whenever there is a continuously differentiable but fast change of the reference signal with 5 N or 40 N difference (for example at $t = 8$ or $t = 20$), the magnitude of the error between the output and the reference force is 4 N at most, and the control input has peaks about 0.08 large at most. However, within 1 second the error is close to a steady state; note that this steady state is positive, which may be due to the experimental set-up. the set-off is much smaller than the predicted $\lambda = 50$ strip in Theorem 4.1.

In Experiment 2, a piecewise constant reference trajectory is applied. This can be viewed as several experiments with constant reference trajectory, where each single experiment is stopped after finite time. Again the position of the piston rod is fixed. As depicted in Figure 8, the peaks of the transient behaviour of the output following the switched constant reference trajectory mirror the hights of the steps and, most importantly, within less than 0.1 seconds the output is within a 1 N neighbourhood of the reference trajectory; the latter is depicted in Figure 6 where we zoomed into the time interval $[7.8, 8.1]$. Again, the actual practical tracking is much better than the conservatives estimates given in Theorem 4.1.

In Experiment 3, we show the effect of an external disturbance changing the position of the piston, i.e. $v \not\equiv 0$; the reference force is set to $y_{\text{ref}} \equiv 0$. Note that the faster the movement of the piston the larger the error. However, although the external disturbances produce an

error of magnitude up to 60 N, the experiment shows that within 2 seconds the output $y(t)$ is within a 1 N neighbourhood of reference force $y_{\mathrm{ref}}(t)$, see Figure 10. A larger gain k in (9) would theoretically yield a smaller error, but additional experiments with larger gains showed unsatisfactory behaviour due to amplifying measurement noise.

6 Conclusions

First, we have introduced a mathematical model for a pneumatic actuator taking into account essential nonlinearities. We have then investigated the mathematical properties of this model and have shown that the mathematical properties of the model coincide with the engineering understanding: the pressure values remain positive, the solution is unique and bounded. Secondly, we have investigated a proportional error feedback control with saturation. Although intuitively clear, it is mathematically not straightforward how to cope with the saturation and the underlying nonlinearities of the model. However, we have proved that practical tracking is achieved under the assumptions that (i) the derivative of the reference signal is limited, (ii) the disturbance, such as the velocity of the piston, is limited, and (iii) the pressures remain in a certain compact set. These assumptions are conservative and needed only for the mathematical proof, but as illustrated by the experimental results, the actual measurements are much more convincing.

Acknowledgement: We are indebted to A. Hildebrandt (TU Ilmenau) for constructive comments and for carefully setting up the experiments and displaying the measurements.

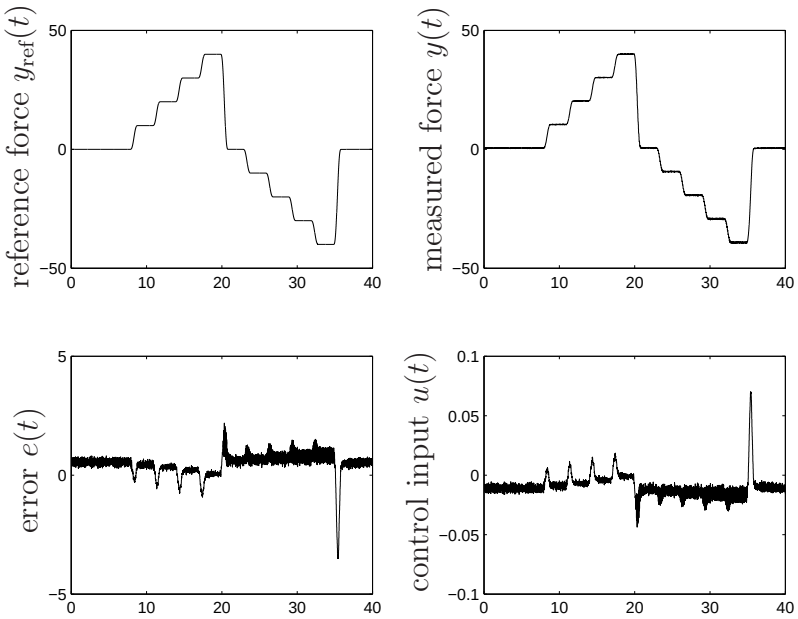

Figure 7: Experiment 1: Force control with continuously differentiable reference signal and fixed piston position.

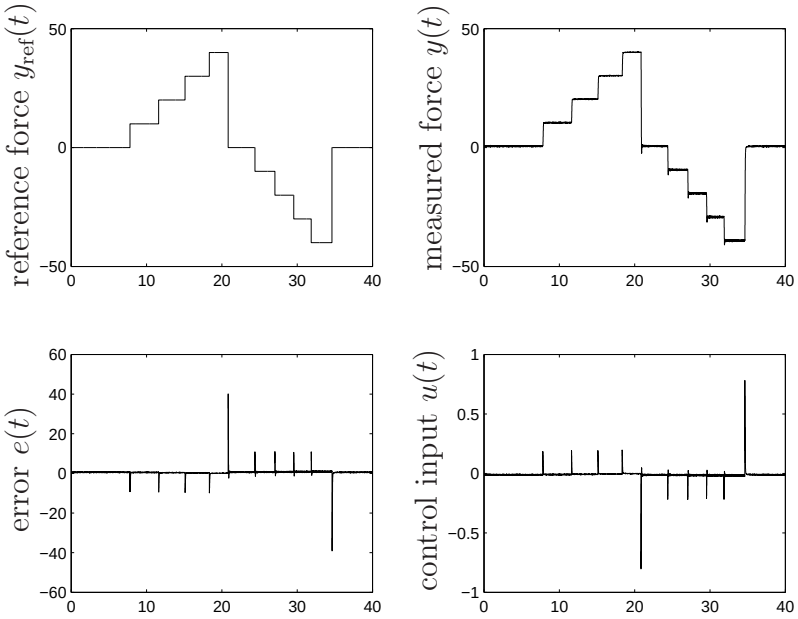

Figure 8: Experiment 2: Step function reference force and fixed position for piston rod.

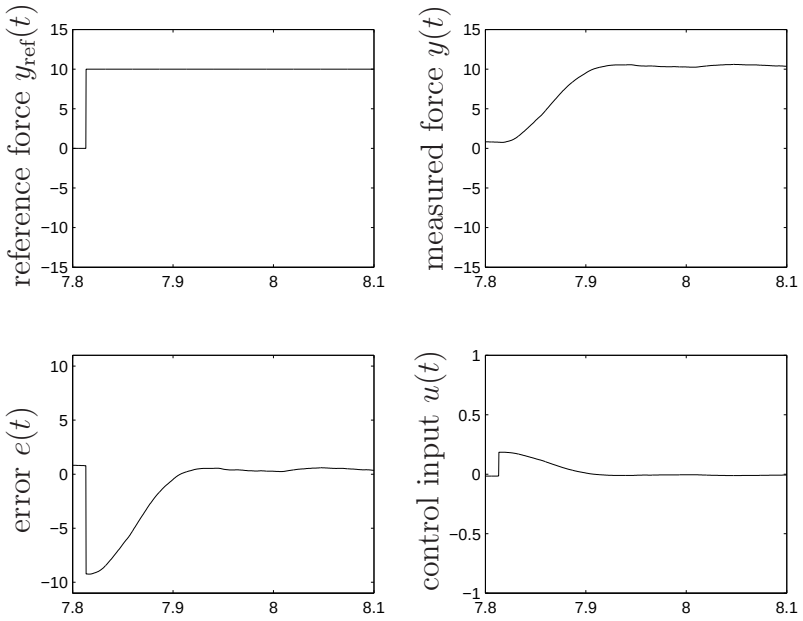

Figure 9: Experiment 2: Zoom of Figure 8.

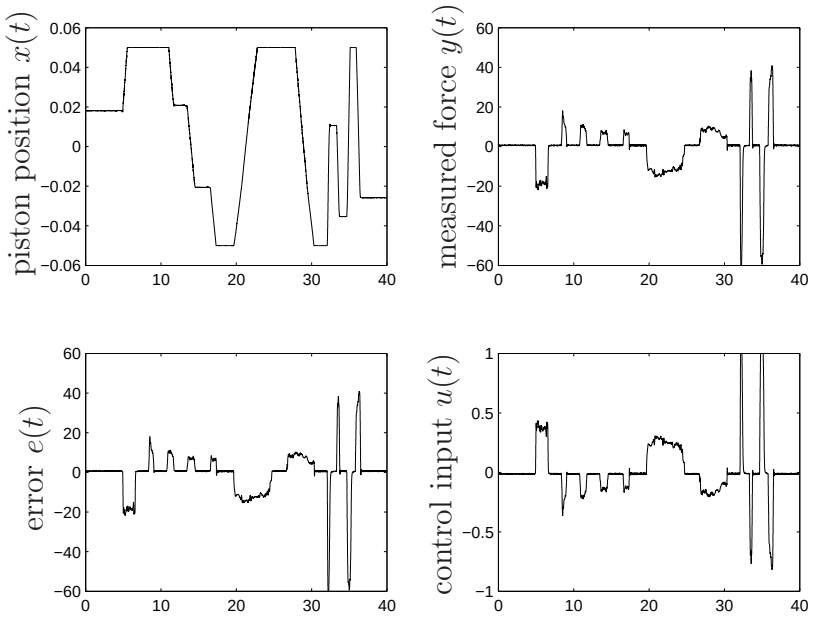

Figure 10: Experiment 3: Force control with reference force $y_{\mathrm{ref}} \equiv 0$ and moving piston.

References

[1] M. Göttert. *Bahnregelung servopneumatischer Antriebe*. PhD thesis, University of Siegen, DE, 2003.

[2] A. Hildebrandt, O. Sawodny, R. Neumann, and A. Hartmann. A flatness based design for tracking control of pneumatic muscle actuators. In *Proc. of the 7th Int. Conf. on Control, Automation, Robotics and Vision (ICARV02)*, pages 1156–1161, Singapore, 2002.

[3] A. Hildebrandt, O. Sawodny, R. Neumann, and A. Hartmann. Cascaded tracking control concept for pneumatic muscle actuators. In *Proc. of the European Control Conference (ECC), CD-ROM*, Cambridge, 2003.

[4] Y.-S. Jeon, C.-O. Lee, and Y.-S. Hong. Optimization of the control parameters of a pneumatic servo cylinder drive using genetic algorithms. *Control Engineering Practice*, 6(7):847–854, 1998.

[5] T. Kimura, S. Hara, and T. Tomisaka. H-infinity control with minor feedback for a pneumatic actuator system. In *Proc. of 35th IEEE Conf. on Decision and Control (CDC)*, volume 3, pages 2365–2370, Kobe, Japan, 1996.

[6] N. Manamanni, M. Djemai, T. Boukhobza, and N.K. M'Sirdi. Nonlinear sliding observer-based control for a pneumatic robot. *Int. J. of Robotics & Automation*, 16(2):100–112, 2001.

[7] D. McCloy and H.R. Martin. *Control of Fluid Power: Analysis and Design*. Ellis Horwood Series in Engineering Science. Wiley, John & Sons, Incorporated, New York, Toronto, 2nd rev. edition, 1980.

[8] O. Ohligschläger. *Pneumatische Zylinderantriebe - thermodynamische Grundlagen und digitale Simulation*. PhD thesis, RWTH Aachen, DE, 1990.

[9] N.-C. Park, H.-S. Yang, H.-W. Park, and Y.-P. Park. Position-vibration control of two-degree-of-freedom arms having one flexible link with artificial pneumatic muscle actuators. *Robotics and Autonomous Systems*, 40(4):239–254, 2002.

[10] M. Parnichkun and C. Hgaecharoenkul. Kinematics control of a pneumatic system by hybrid fuzzy pid. *Mechatronics*, 11(8):1001–1024, 2001.

[11] O. Sawodny and A. Hildebrandt. Aspects of the control of differential pneumatic cylinders. In E. Shimemura and M. Fujita, editors, *Proc. of German-Japanese Seminar*, pages 247–256, Noto Hanto, 2002.

[12] H. Schulte and H. Hahn. Fuzzy state feedback gain scheduling control of servopneumatic actuators. *Control Engineering Practice*, 12(5):639–650, 2004.

[13] M.C. Shih and M.A. Ma. Position control of a pneumatic cylinder using fuzzy pwm control method. *Mechatronics*, 8(3):241–254, 1998.

[14] M.C. Shih and S.-I. Tseng. Identification and position control of a servo pneumatic cylinder. *Control Engineering Practice*, 3(9):1285–1290, 1995.

[15] E.D. Sontag. *Mathematical Control Theory*. Springer-Verlag, New York and others, 2nd edition, 1998.

[16] K. Tanaka, Y. Yamada, T. Satoh, A. Uchibori, and S. Uchikado. Model reference adaptive control with multi rate neural network for electro pneumatic servo system. In *Proc. of IEEE Conf. on Control Applications (CCA)*, pages 1716–1721, Hawaii, 1999.

[17] J. Wang, J. Pu, and P. Moore. A practical control strategy for servo-pneumatic actuator systems. *Control Engineering Practice*, 7(12):1483–1488, 1999.

[18] T. Wey, M. Lemmen, and W. Bernzen. Hydraulic actuators for flexible robots: A flatness based approach for tracking and vibration control. In *Proc. of the European Control Conference (ECC), CD-ROM*, Karlsruhe, 1999.

[19] F. Xiang and J. Wikander. Block-oriented approximate feedback linearization for control of pneumatic actuator system. *Control Engineering Practice*, 12(4):387–399, 2004.